


β -1,3-D-Glucan Schizophyllan/Poly(dA) Triple-Helical Complex in Dilute Solution

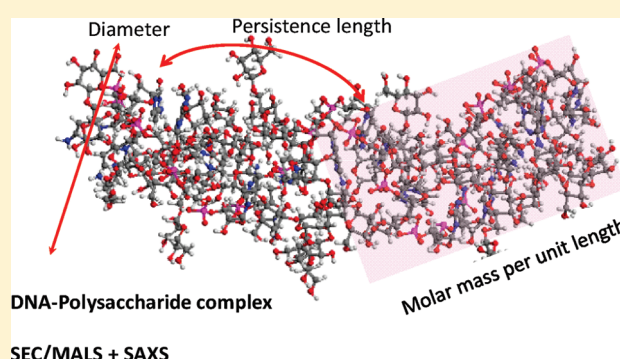
Yusuke Sanada,[†] Tsubasa Matsuzaki,[†] Shinichi Mochizuki,[†] Tadashi Okobira,[‡] Kazuya Uezu,[†] and Kazuo Sakurai^{*,†}

[†]Department of Chemistry and Biochemistry, University of Kitakyushu, Hibikino, Kitakyushu 808-0135, Japan

[‡]Fukuoka Industry, Science & Technology Foundation, Acros Fukuoka Nishi Office 9F, 1-1-1, Tenjin, Chuo-ku, Fukuoka 810-0001, Japan

 Supporting Information

ABSTRACT: A certain length of poly(deoxyadenylic acid) (dA_x) can form a novel complex with β -1,3-D-glucan schizophyllan (SPG) with a stoichiometric composition of one dA binding two main chain glucoses. We measured dilute solution properties for the complex with light and small-angle X-ray scattering as well as intrinsic viscosity and found that the complex behaves as a semiflexible rod without branching or cross-linking. We analyzed the data with the wormlike cylinder model, and the chain dimensions and the persistence length for the complexes were consistently determined. The chain flexibility was reduced to almost 25% upon complexation for dA/SPG and to 15% for S-dA/SPG, where S-dA denotes the phosphorothioated DNA analogue. The changes in the molar mass per unit length and the diameter indicated that the helix was elongated or stretched along the axis direction upon the complexation.



INTRODUCTION

Schizophyllan (SPG) is an extracellular polysaccharide produced by the fungus *Schizophyllum commune* and consists of linearly linked β -1,3-D-glucose with one β -1,6-D-glucose side chain for every three main chain glucoses (Figure 1).^{1,2} It dissolves in neutral water as a rodlike triple-helix (tSPG), whereas it disperses as a single chain (sSPG) in dimethyl sulfoxide (DMSO) and alkaline solutions (>0.25 N NaOH).^{3–5} Recurrence of tSPG, similar to renaturation for proteins, is observed when the solution conditions of sSPG are changed to those favoring for tSPG such as pH = 5–8 or DMSO/water <4 (weight). Although the local conformation for the renatured SPG obtains indeed the same triple helix of the natural one, according to X-ray diffraction patterns,^{6,7} there are observed many branches or cross-links for its overall morphology, depending on the renaturation concentrations.⁸ Circular objects are sometimes formed as the result of the intramolecular end-to-end interactions of sSPG chain when the renaturation is carried out in dilute concentrations.^{9,10} A singular aspect of this polysaccharide is the formation of a novel polysaccharide/polynucleotide complex (Figure 1). When single-chain homopolynucleotides such as poly(cytidylic acid) (poly(C)) and poly(deoxyadenylic acid) (poly(dA)) are present in the renaturation process, a new complex is formed instead of the formation of tSPG.^{11,12} The formation of polysaccharide/polynucleotide complexes is thermodynamically more favorable than that of tSPG. This is because

the addition of poly(dA) to the renatured tSPG solution can induce the formation of the complex. Later, it is shown that this complexation ability is generally observed for the β -1,3-D-glucan family including zymosan.¹³ Until now, no heterosequence of DNA nor RNA has been found to bind to SPG. The complex has an exact stoichiometric composition that two main chain glucoses bind with one nucleotide, presumably with the combination of the hydrogen bonds and hydrophobic interactions. By use of this complexation and the biological recognition of SPG with a cellular receptor called dectin-1, the complex is used as a delivering vehicle for therapeutic oligonucleotides including antisense and CpG DNAs to the antigen presenting cells that express dectin-1.^{14–16}

Among polynucleotides, poly(dA)_x shows the highest binding affinity to SPG, and when the number of dA/X exceeds about 40, the complexation yield become close to 100%. Recently, it was found that the binding stability is further enhanced by phosphorothioation of the polynucleotide backbone of poly(dA), denoted by S-dA_x.^{16,17} These findings enable accurate molecular characterizations of the complexes in solution by use of scattering techniques, because the conformational analysis with scattering generally requires the single-component system. Our very first work with the small-angle X-ray scattering (SAXS)¹² was done for a poly(C)_x/SPG complex, where

Received: September 19, 2011

Revised: November 16, 2011

Published: November 16, 2011

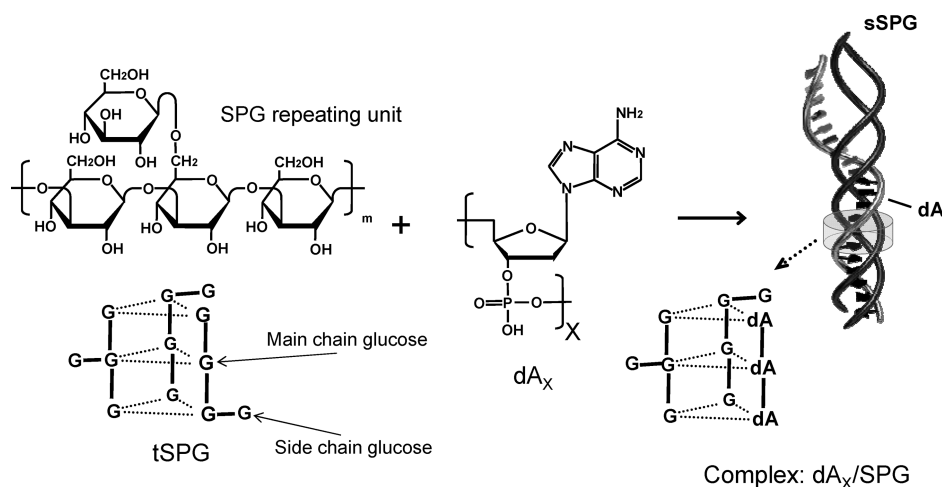


Figure 1. Repeating unit of schizophyllan (SPG) and poly(deoxyadenylic acid)(dA_X) and an illustration of their complexation and stoichiometric structures of the triple helix of SPG and the complex, denoted tSPG and dA_X/SPG.

X is 200–300 due to enzymatic polymerization. Although such a long polynucleotide is considered to preferably form the complex, we have to admit ambiguity in the characterization because we did not examine the complexation yield.

Dilute solution properties of tSPG and its conformation have been extensively studied by Norisuye and co-workers for carefully fractionated samples with a wide range of the molecular weight,^{3–5,18,19} and it was revealed that tSPG in aqueous solution is well-described with the wormlike cylinder model with the persistence length, denoted by p , of 150–200 nm, the hydrodynamic diameter of 2.6 ± 0.4 nm, and the molar mass per unit length of $2150\text{--}2170\text{ nm}^{-1}$. In comparison with other semiflexible polymers, tSPG is rather stiff; for example, p of the double strand of DNA is 60–70 nm.²⁰ Later, Yanaki et al.²¹ showed that scleroglucan, having the same chemical structure as SPG but obtained from a different source, shows the almost identical dilute solution properties with tSPG. Sletmoen and co-workers^{22,23} carried out size exclusion chromatography coupled with multiangle light scattering (SEC/MALS) and atomic force microscopy (AFM) for the complex made from scleroglucan and poly(C). From the molecular weight dependence of the radius of gyration determined with static light scattering, denoted by $\langle S^2 \rangle^{1/2}$, they concluded that the scleroglucan/poly(C) complex takes a linear-rodlike conformation and has a higher persistence length than the original scleroglucan. However, it may seem that their chromatogram main peak contains multiple components.

The first task of this paper is to examine whether the solution only contains the complex when it is made at an appropriate condition to do so. The second is to measure the dilute solution properties of SPG/poly(dA) complexes, combining synchrotron SAXS and SEC/MALS as well as SEC/viscometer, and determine the conformational parameters. These parameters directly reflect in situ behavior of complexes, which cannot be obtained from microscopic study. These results are fundamentally important to understand the physical chemistry of the complexes, as well as being necessary to apply the complex to therapeutics and to obtain approval for practical use.

EXPERIMENTAL SECTION

Materials. The two samples of triple helix of SPG were kindly provided by Mitsui Sugar Co., Ltd. (Tokyo, Japan), and the

reported weight-averaged molecular masses (M_w) were 4.5×10^5 and 1.1×10^6 g/mol, respectively. Phosphorothioate and phosphodiester dA₆₀ and dA₁₀₀ were synthesized at FASMAC Co., Ltd. (Kanagawa, Japan), and the molar masses (M) of these samples are 1.87×10^4 (dA₆₀), 2.06×10^4 (S-dA₆₀), 3.12×10^4 (dA₁₀₀), and 3.43×10^4 (S-dA₁₀₀) g/mol, respectively, where the phosphorothioated dA was denoted S-dA to distinguish it from phosphodiester one. Poly(dA) was purchased from Sigma, where the number of dA was determined with gel electrophoresis to be 250–350 ($M_w = 7.8\text{--}10.9 \times 10^4$) and it was found that its distribution was rather broad due to enzymatic polymerization.

Complexation and Renaturation. In the complex, two main chain glucoses bind to one dA, as presented in Figure 1. We prepared the complexes in this stoichiometric composition of 2:1 and also in a nucleotide excess composition of 3:1. The X-ray and light scattering intensities are more amplified from larger particles than from smaller ones. Therefore, uncomplexed (free) dA may not provide significant signals in the scattering experiments, whereas uncomplexed SPG might do. This is the reason that we additionally chose the nucleotide excess composition. As we described later, even when we mixed at the stoichiometric composition, we observed both free dA₆₀ and free SPG coexisting with dA₆₀/SPG complex, whereas S-dA₆₀/SPG showed almost no free dA when it was prepared in the stoichiometric ratio.

The typical procedure for the complex formulation is as follows. The fixed amount of tSPG was dissolved in 0.25 N NaOH(aq) for more than 2 days to completely dissociate the triple helix to the single chains. An appropriate amount of sSPG solution, dA_X in water, and a phosphate buffer solution (330 mM NaH₂PO₄, pH 4.7) were mixed. After mixing, pH was controlled around 7 and the solutions were stored at 4 °C for one night. We only used SPG with $M_w = 4.5 \times 10^5$ for conformation analysis since the complex made from the larger M_w was found to contain branches and thus was not suitable for accurate analysis. The renaturation of sSPG was carried out in the similar manner.

Purification of the Complex. After dA₆₀/SPG was prepared even at the nucleotide excess composition, there still remained some amount of uncomplexed SPG in the solutions, coexisting with the complex and free dA₆₀. The uncomplexed SPG was separated with an anion-exchange column [Macro-Prep EDAE, ligand—NH⁺(C₂H₅)₂, 1 mL, BioRad]. First, the mixture was

poured into the column to allow free DNA and the complex to be adsorbed on the column. After a few minutes, free SPG was eluted out with PBS buffer. After this process, we eluted out the adsorbed DNA and complex with 1 M Tris buffer (pH = 7.6).

Light Scattering and Viscometry Measurements. Light scattering and viscosity measurements were carried out by use of a Dawn-Heleos-A (Wyatt) and a ViscoStar-II (Wyatt), respectively, coupled with a Shodex GPC-101 system. An amount of 400 μL of unfiltered solution was injected into a system consisting of a Shodex HPLC pump (DU-H2130) equipped with a Shodex degassing unit (ERC-3125S). The chromatogram was measured with an RI-71S interferometric differential refractive index detector (Shodex) and a UV absorbance detector SPD-10A (Shimadzu). These detectors were connected in series, with the refractometer last because of backpressure. The separation column was consisting of a series of SB-806MHQ and SB-802.5MHQ; both are poly(glyceropropyl methacrylate) gel, and their exclusion limits are 2×10^7 and 7×10^3 for pullulan, respectively, and are maintained at 30.0 $^\circ\text{C}$. The mobile phase was a 50 mM phosphate buffer containing 0.5 M KCl (pH = 7.4) at 0.8 mL/min. The MALS detectors were calibrated with toluene. Data acquisition and manipulation were performed using Wyatt's ASTRA for Windows software (V. 4.73.04). Scattered light intensities at the scattering angles over 14–163 $^\circ$ were measured, and their angular dependence was analyzed using a Berry's plot to determine the radius of gyration ($\langle S^2 \rangle^{1/2}$) and the weight-averaged molecular mass (M_w).

The specific refractive index increment ($\partial n/\partial c$) of dA_{60} and S-dA_{60} in the phosphate buffer were 0.163 and 0.164 $\text{cm}^3 \text{g}^{-1}$, respectively, determined with a DRM-1021 differential refractometer (Otsuka Electronics) at 633 nm and 25 $^\circ\text{C}$ (see the Supporting Information, S1). For the complexes, $\partial n/\partial c$ was calculated from the relation

$$\partial n/\partial c = w_{\text{SPG}}(\partial n/\partial c)_{\text{SPG}} + (1 - w_{\text{SPG}})(\partial n/\partial c)_{\text{dA}} \quad (1)$$

where w_{SPG} is the weight fraction of SPG in the stoichiometric complex. For $\text{S-dA}_{60}/\text{SPG}$ and $\text{dA}_{60}/\text{SPG}$ complexes, w_{SPG} was 0.510 and 0.522, respectively.

Synchrotron SAXS Measurements. SAXS measurements were performed at BL-40B2 of SPring-8, Japan. A 30 cm \times 30 cm imaging plate (Rigaku R-Axis VII) detector was placed at 0.70 or 4.3 m away from the sample position. The wavelengths of the incident beam, denoted by λ , were 0.071 or 0.100 nm. The 0.70 and 4.3 m setups provided the q range of 0.07–5.00 and 0.02–2.00 nm^{-1} , respectively, where q is the magnitude of the scattering vector defined by $q = 4\pi/\lambda \sin(\theta)$ with the scattering angle of 2θ . A bespoke SAXS vacuum sample chamber²⁴ was used, and the X-ray transmittance of the samples was determined with an ion chamber located in front of the sample and a Si photodiode for X-ray (Hamamatsu Photonics S8193) behind the sample.

Wormlike Chain Model. The wormlike cylinder model envisions a continuously flexible and isotropic rod, particularly suited to describe semiflexible polymer chains in solutions, such as tSPG and the double helix of DNA. The physical parameters to characterize the model are the persistence length (p) determined by the bending energy divided by the Boltzmann factor, the molar mass per unit length (M_L), and the cross-sectional diameter of the cylinder (d). The persistence length is an indication of the chain stiffness; it goes to zero for the Gaussian chain and to infinity for the rigid rod limit. The values of M_L and

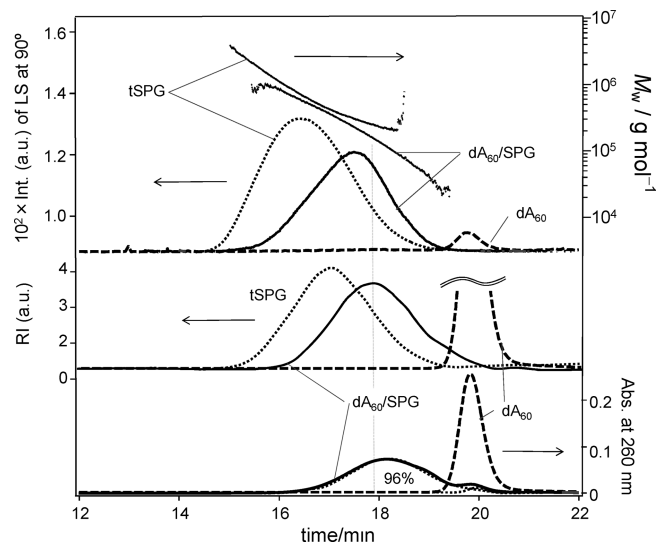


Figure 2. SEC chromatograms for tSPG ($M_w = 4.5 \times 10^5$), dA_{60} ($M = 1.87 \times 10^4$), and $\text{dA}_{60}/\text{SPG}$ prepared at the stoichiometric composition. From the top, the weight-averaged molecular weight, the scattering intensity at 90 $^\circ$, the refractive index signal, and the UV absorbance at 260 nm are shown. The UV chromatogram for $\text{dA}_{60}/\text{SPG}$ was deconvoluted to two Gaussians to represent the complex and free DNA, and each deconvoluted line is shown as a dotted line (indicated by arrow).

d are well-related to the molecular dimension and the chemical structures.^{20,25–27}

The radius of gyration of a wormlike chain with the contour length of L and the persistence length of p can be written with the Benoit–Doty equation in the case of $L \gg d$.

$$\langle S^2 \rangle = \frac{pL}{3} - p^2 + \frac{2p^3}{L} \left[1 - \frac{p}{L} (1 - e^{-L/p}) \right] \quad (2)$$

The contour length is related to the molecular weight of the chain by $L = M/M_L$. At the rod limit, the relation of $(12)^{1/2} \langle S^2 \rangle^{1/2} = M/M_L$ is held. Light scattering experiments give the set of $\langle S^2 \rangle^{1/2}$, and M_w and fitting the data with this equation can provide the persistence length p .

As the hydrodynamic theory for wormlike chains, Yamakawa and co-workers^{20,26,28} formulated for the intrinsic viscosity ($[\eta]$) for a wormlike cylinder that its centroid obeys the statistics of the wormlike chain and has a hydrodynamic diameter of d_h . Although $[\eta]$ cannot be analytically expressed, they provided an empirical table to calculate $[\eta]$ as a function of L , M_L , p , and d_h , except for short flexible cylinders. It is known that the value of d_h usually gives a very close value to that determined with other methods such as crystallography.^{3–5}

SAXS measurements give the scattering function so-called form factor that represents the local conformation of polymer chains. The scattering function of a wormlike cylinder can be expressed as follows:

$$I(q) \propto L^{-2} \int_0^L (L-x) F(\vec{q}; x) dx \quad (3)$$

Here, $F(\vec{q}; x)$ can be expressed as the Fourier transform of the probability density function that the contour point x is found at a specified point (which can be related to \vec{q}) and may be expanded with the moments. Nakamura and Norisuye²⁹ calculated these moments and obtained a series of numerical tables that allow us

to calculate the form factor for the entire q range as a function of p , L , and d .

RESULTS

Chromatography. Figure 2 shows SEC chromatograms for tSPG, dA₆₀/SPG (prepared at the stoichiometry), and dA₆₀ detected with an LS photodiode at $2\theta = 90^\circ$ (upper left), the RI refractometer (middle left), and the UV spectrometer at $\lambda = 260$ nm (bottom right). The weight-averaged molar mass was determined for each sample and plotted against the elution time (upper right). Since tSPG has no absorption at 260 nm, whereas dA has, UV chromatograms were only observed for dA₆₀/SPG and dA₆₀. For the main peaks of dA₆₀/SPG in the RI and UV chromatograms, the peak-top positions and their shapes were very similar but not identical: the RI peak was eluted more forward (i.e., higher molecular weight) than the UV peak and showed tailing to the low molar-mass side. This fact indicates that uncomplexed SPG was mixed with the dA₆₀/SPG complex in the main peak. The UV showed a small secondary peak at 20 min with the same position as dA₆₀ alone, meaning the presence of uncomplexed dA₆₀. When this bimodal peak was deconvoluted with two Gaussians representing dA₆₀/SPG and dA₆₀ (dotted lines in the UV chart of Figure 2), the complexation yield was estimated to be 96%. When the sample was prepared at a dA₆₀ excess composition of 3:1, the UV and RI became less different, while the amount of uncomplexed dA was increased along with the composition (data not shown). This result can be interpreted by that main peak contained less free SPG and the composition was almost uniform in the main peak. Therefore, we used the dA excess composition for further analysis for the all phosphodiester complexes.

When we carried out the same experiment for S-dA₆₀/SPG, we observed that the stoichiometric sample had no free S-dA₆₀ and the complexation yield was almost 100% (see the Supporting Information, S2). The peak top appeared at 17 min, becoming more forward than dA₆₀/SPG (18 min) and close to tSPG (16.2 min), indicating that S-dA₆₀/SPG shows a higher complexation yield than dA₆₀/SPG. For dA₁₀₀ and poly(dA), the complexation yield was also close to 100%.

For poly(dA)/SPG, the peak position was shifted toward the larger molar-mass side when the concentration of the sSPG in alkaline solution was increased. Furthermore, when the sSPG concentration was above 5 mg/mL, insoluble gel-like particles, presumably made from renatured SPG, were formed after being mixed with the poly(dA) solution, and the complex yield was decreased. On the other hand, dA₁₀₀ and dA₆₀ in both phosphodiester and phosphorothioate showed that the peak position did not depend on the sSPG concentration.

Figure 2 shows that the molar masses of tSPG at the LS peak top is 4.0×10^5 . This value is larger than that of the complex (2.0×10^5). For the other samples, tSPG always showed a larger molar mass than the complexes, except for poly(dA)/SPG. As mentioned in the Introduction, it is considered that one dA binds to two main chain glucoses in the different sSPG chains (see Figure 1). This means that one-third of the tSPG chain is replaced by dA_x chains. Considering the difference in the molar mass between glucose and deoxyadenosine monophosphate (163 and 312, respectively), the molar mass of the complex should become larger than the original tSPG by the factor of 1.15. In the experiments, however, the complex showed a smaller molar mass. We suppose that this decrease can be ascribed to the

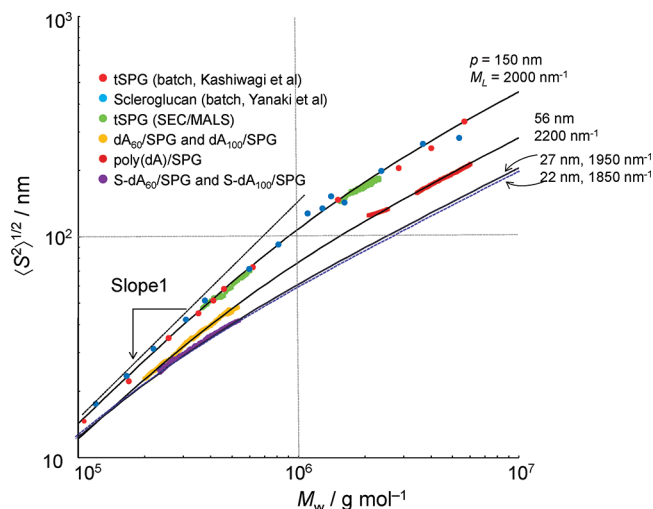


Figure 3. Comparison of the measured and reported $\langle S^2 \rangle^{1/2}$ for tSPG and scleroglucan with those of the complexes of dA₆₀/SPG, dA₁₀₀/SPG, S-dA₆₀/SPG, S-dA₁₀₀/SPG, and poly(dA)/SPG. The solid lines fitted to the data are calculated from the Benoit–Doty equation with the indicated parameters.

presence of a nick of the single SPG chain consisting tSPG or to chain scission occurred during the dissociation of tSPG in alkaline solution. If there is such a nick or scission, M_w of sSPG would be smaller than one-third of tSPG, and thus the resultant complex also would show a smaller molar mass than expected.

To summarize the results of the chromatography, when the samples were made at the stoichiometry for S-dA₆₀ and S-dA₁₀₀ and at the DNA rich for dA₆₀ and dA₁₀₀, the main peak was considered to mainly consist of the complex. Hereinafter, we use these fractions for conformation analysis. We can take out uncomplexed SPG from the main peak by use of an anion-exchange column, as shown below. However, since the purified complexes give the same results, we did not apply the purification to all samples.

Molecular Mass Dependence of the Radius of Gyration. The radius of gyration $\langle S^2 \rangle^{1/2}$ is plotted against M_w for all samples in Figure 3, comparing the batch measurements for tSPG by Kashiwagi et al.,⁴ including the data for scleroglucan.²¹ Since SPG and scleroglucan have the same chemical structure but different fungus sources, both data points agree with each other. Our data for the two tSPG samples coincide with those for the batch measurements. Since there was no significant difference between dA₆₀/SPG and dA₁₀₀/SPG for both DNA types, these are not discriminated. Most of measurements were repeated three or four times, and the data were averaged.

The solid lines fitted to the data points of tSPG and scleroglucan were calculated from eq 2 with $p = 150$ nm and $M_L = 2000$ nm^{−1}. As Nakamura et al.²⁹ showed, the data points were well-reproduced by the wormlike chain model in the range of 2 orders of the magnitude of $\langle S^2 \rangle^{1/2}$. Compared with tSPG at the same $\langle S^2 \rangle^{1/2}$ values, dA₆₀/SPG was shifted toward the larger molecular weight side and S-dA₆₀/SPG was shifted furthermore and the slope was decreased. The slope of dA₆₀/SPG is almost parallel with that of tSPG. At low- M_w regions, $\langle S^2 \rangle^{1/2}$ is mainly determined by M_L , as expressed by $(12)^{1/2} \langle S^2 \rangle^{1/2} = M/M_L$. Therefore, the shift can be interpreted by increase of M_L upon the complexation. Assuming that poly(dA)/SPG has the same wormlike chain parameters with dA₆₀/SPG and dA₁₀₀/SPG,

Table 1. Wormlike Chain Parameters

		p/nm	M_L/nm^{-1}	d or d_h/nm	h/nm	ref
tSPG	$\langle S^2 \rangle^{1/2a}$	150 ± 30	2000 ± 50		0.30	Kashiwagi et al. (ref 4)
	$[\eta]$	200 ± 30	2150 ± 150	2.6 ± 0.2	0.30	Yanaki et al. (ref 18)
	SAXS	170 ± 20		2.6 ± 0.1		Sakuragi et al. (ref 30)
	X-ray		2000	1.86	0.29	Deslandes et al. (ref 6)
	MD		1951	2.65	0.290	Miyoshi et al. (ref 31)
dA/SPG	$\langle S^2 \rangle^{1/2}$	56 ± 3	2200 ± 50		0.34	
	$[\eta]$	40 ± 2	2000 ± 50	2.2 ± 0.3	0.37	
	SAXS	55 ± 5		2.4 ± 0.1		
	MD		2170	3.05	0.306	Okobira et al. (ref 32)
S-dA/SPG	$\langle S^2 \rangle^{1/2}$	25 ± 5	1900 ± 100		0.40	
	$[\eta]$	18 ± 2	1900 ± 50	2.4 ± 0.3	0.40	
	SAXS	35 ± 10		2.5 ± 0.1		
	MD		2050	2.94	0.325	Okobira et al. (ref 32)

^aWe reanalyzed the data combined with tSPG and scleroglucan, adding our SEC/MALS data, and obtained $p = 130$ nm and $M_L = 1950$ nm.

from the fitting data with eq 2, we can obtain the best combination of $p = 56 \pm 5$ nm and $M_L = 2200 \pm 100$ nm⁻¹. This fitting, indeed, shows that M_L is increased by the complexation and the chain becomes more flexible. For S-dA₆₀/SPG and S-dA₁₀₀/SPG, the slope is about 0.7, and thus the contribution from p cannot be ignored. By fitting we determined that $p = 25 \pm 6$ nm and $M_L = 1900 \pm 150$ nm⁻¹. Since we do not have the larger molecular mass data for S-dA_x/SPG, the error inevitably enlarges. Although the large error for fitting, the M_L values more than 2000 nm⁻¹ could not fit the data with any combination of p . The allowable range for the determination was found to be 20–30 nm for p and 1800–2000 nm⁻¹ for M_L ; the calculated lines with $p = 27$ nm and $M_L = 1950$ nm⁻¹ and $p = 22$ nm and $M_L = 1850$ nm⁻¹ are depicted in the figure for comparison. The results of the determined parameters are summarized in Table 1.

To sum up the fitting analysis, dA_x/SPG showed a larger M_L and smaller p than tSPG, whereas S-dA_x/SPG decreased both M_L and p . If one-third of tSPG is replaced by dA or S-dA without conformational changes, M_L would be increased by 1.15 and 1.17 times, respectively. The decreased M_L suggests that this assumption is not correct and the complexation may stretch the pitch of the triple helix of the complex.

Small-Angle X-ray Scattering to Determine p and d .

Figure 4 presents SAXS profiles for tSPG, dA₆₀/SPG, and S-dA₆₀/SPG, after connecting the data for two different camera lengths (4.3 and 0.7 m) and extrapolating them to the zero concentration. For dA₆₀/SPG and S-dA₆₀/SPG, the measured concentrations were 0.325, 0.500, and 1.01 mg/mL and the concentration dependence of $I(q)$, i.e., the dense packing effect,³³ became appreciable in the range of $q < 0.2$ nm⁻¹. For tSPG, the concentrations had to be increased to 0.801 and 1.625 mg/mL because saccharide has a lower electron density difference in water than polynucleotide. All the data showed the relation of $I(q) \propto q^{-1}$ in the middle range, which is expected for rigid thin rods, and the intensity deviated upward at the low- q and downward in the high- q regions. The former deviation is ascribed to chain flexibility, and the latter downward deviation is caused by the finite size of the cross section of the chain. From these deviations, the persistence length and the diameter of the wormlike cylinder can be determined, respectively.

To compare the data with the Norisuye–Nakamura theory, we replotted the data as the Holtzer plot, and Figure 5 presents

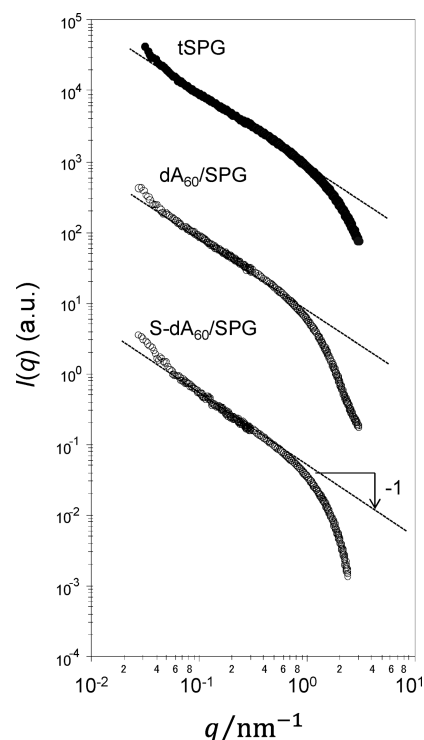


Figure 4. Small-angle X-ray scattering profiles after being extrapolated to the zero concentration for tSPG, dA₆₀/SPG, and S-dA₆₀/SPG.

that of dA₆₀/SPG, for example. The right plot shows the entire q range, and the low- q range was enlarged in the left panel. By fitting the data with the Norisuye–Nakamura theory, p and d can be determined to be $d = 2.4 \pm 0.2$ nm and $p = 55 \pm 5$ for this case. For the other samples, the parameters were determined, and all of the results are summarized in Table 1. The p values determined from SAXS are slightly larger than those from $\langle S^2 \rangle^{1/2}$ for tSPG and S-dA_x/SPG, whereas it is the same for dA/SPG, although they are in agreement within error range.

Molecular Weight Dependence of Intrinsic Viscosity. Figure 6 plots $[\eta]$ against M_w for dA₆₀/SPG and S-dA₆₀/SPG, comparing with that of tSPG. As Yanaki et al.¹⁸ showed, the data points for M_w lower than 5×10^5 are fitted by a straight line with

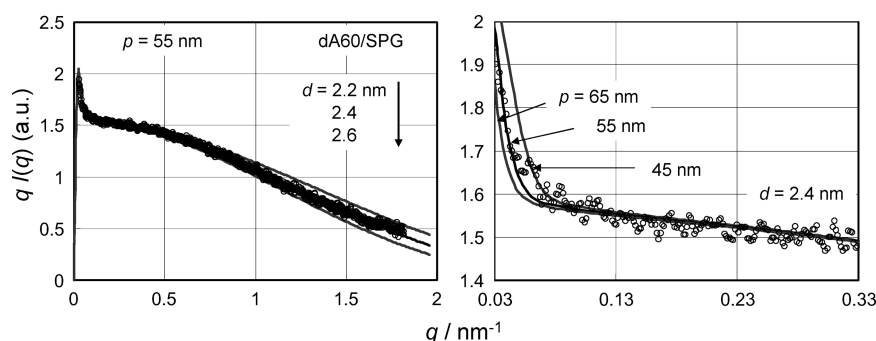


Figure 5. Holtzer plots for the SAXS data of dA60/SPG, compared with the Norisuye–Nakamura theory with different parameters.

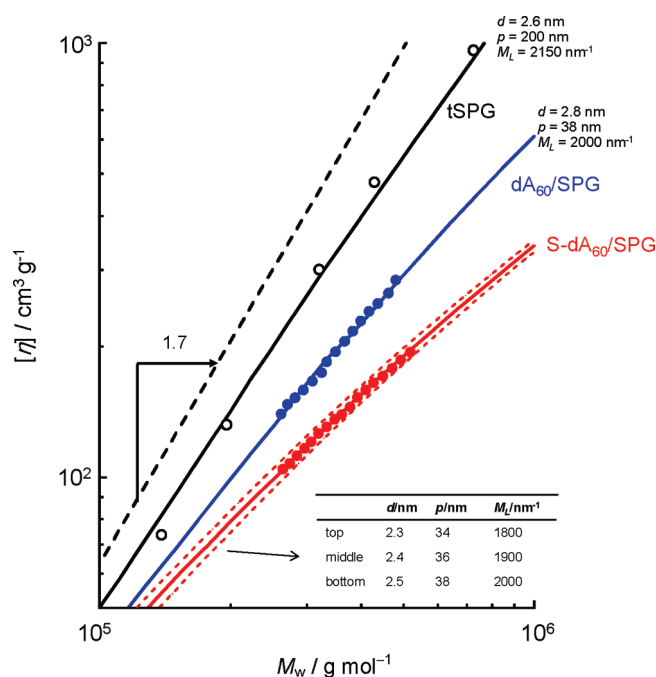


Figure 6. Molecular weight dependence of the intrinsic viscosities for tSPG, dA₆₀/SPG, and S-dA₆₀/SPG, compared with the calculated values from the Yamakawa theory with the indicated parameters.

the slope of 1.7. This slope is confirming that tSPG behaves as a rigid rod in this molecular weight range. For dA₆₀/SPG, compared with SPG at the same $[\eta]$, the data points shifted toward the large M_w and the slope was tilted to 1.6. For S-dA₆₀/SPG, the data points further shifted and the slope became almost 1.4. Again, dA₁₀₀/SPG and S-dA₁₀₀/SPG showed almost the same values as dA₆₀/SPG and S-dA₆₀/SPG; these are not presented.

The Yamakawa theory for $[\eta]$ of a long rigid rod with the hydrodynamic diameter (d_h) predicts $[\eta] \propto (M_L)^{-1} L^2 / \ln(L/d_h)$. Infinitely long thin rigid rods give the relation of $[\eta] \propto L^2$, and such asymptotic behavior can be only observed in the case of $L/d_h \gg 10^3$. However, for real semiflexible chains, when the axial ratio reaches such a large number, the finite flexibility becomes substantial in determining $[\eta]$, which normally decreases the scaling factor of α in $[\eta] \propto L^\alpha$. In the small axial ratios, d_h decreases α . Therefore, there is a rare case to give $\alpha = 2$. In fact, $\alpha = 1.7$ can be obtained for the lower molecular weight region, by substituting $M_L = 1900 \text{ nm}^{-1}$ and $d_h = 2.2 \text{ nm}$ to the equation of $[\eta] \propto (M_L)^{-1} L^2 / \ln(L/d_h)$ and the resultant values well-reproduce

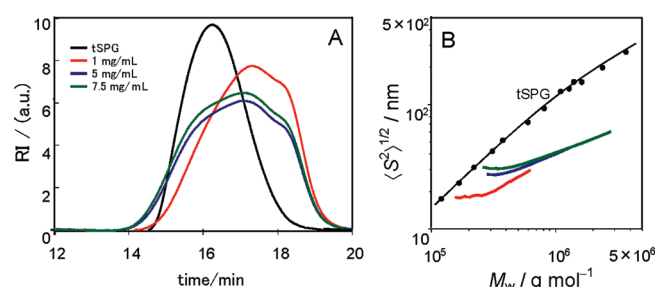


Figure 7. SEC chromatograms for renatured SPG with different concentrations (A) and the corresponding plots for $\langle S^2 \rangle^{1/2}$ against M_w compared with that of tSPG (B).

the M_w dependence of $[\eta]$ for tSPG at $M_w < 5 \times 10^5$. Comparing this dependence, the complex's results suggest that there is an increase in d_h and decrease in M_L and p compared with tSPG. The combinations of the parameters determined by fitting are summarized in Table 1, and the resultant theoretical curves are presented in the figure. To clarify the error range, three lines are presented for S-dA₆₀/SPG with different combinations of the parameters.

Renatured and Uncomplexed SPG. Figure 7A presents the RI chromatograms for renatured SPG with three different concentrations of sSPG in the alkaline solution. With decreasing concentration, the chromatogram peak shifted to longer elution time. The peak widths were broader than tSPG, and their shapes do not look like that of single distribution, suggesting the presence of multiple modes of the renaturation. These results are in strong contrast to the fact that the complexation with the short DNAs (dA₆₀ and dA₁₀₀) gave bare SPG concentration dependence in the chromatogram. Panel B of Figure 7 plots $\langle S^2 \rangle^{1/2}$ for these samples. For all samples, at lower M_w , the slopes were almost zero, and they increased with increase of M_w and finally reach $\langle S^2 \rangle^{1/2} \propto M_w^{0.4}$. When we observed AFM for these samples, the samples contained cross-linked rods, isolated branched rods, and circular objects. We presume that these mixed architectures gave the broad and complex peaks as shown in panel A of Figure 7.

Figure 8A compares the RI chromatograms for tSPG, purified dA₆₀/SPG with the anion-exchange column, and the free SPG that was not adsorbed by the column (denoted by “column-through”). In this case, the complexation was carried out at the DNA-rich composition. The free SPG appeared at the surprisingly low molecular weight region, i.e., from 9×10^4 to 2.0×10^5 , and M_w at the peak top was 1.3×10^5 . Since M_w of tSPG (at the peak top) was 4.0×10^5 , it is suggested that the free SPG almost consists of individual chains of SPG. When we observed AFM

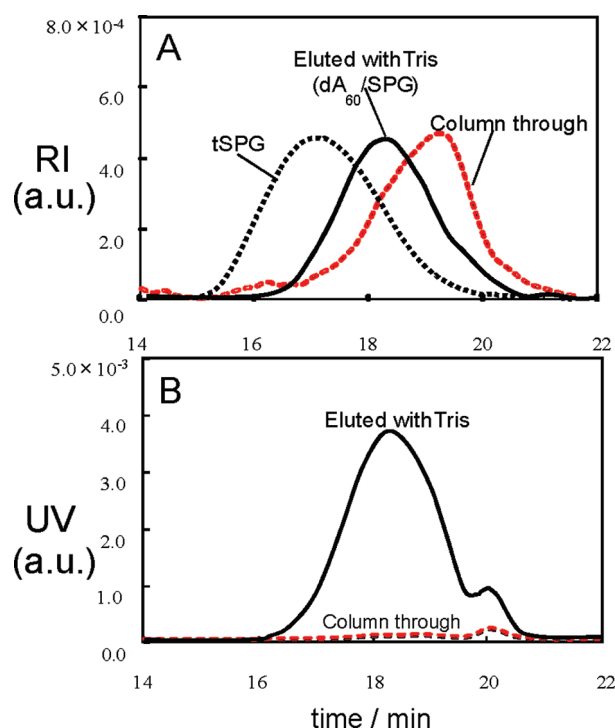


Figure 8. Comparison of SEC chromatograms between tSPG, the fraction adsorbed on the column and then eluted with Tris buffer (dA₆₀/SPG), and the column-through fraction (free SPG) (A and B).

for the column-through fraction, we found circular or ellipsoidal objects as presented in the Supporting Information (S3). According to the previous work,^{9,10} these circular objects are the result of the intramolecular end-to-end interactions of single SPG chains. Therefore, we presume that once SPG forms such an intramolecular binding, it never interacts with dA, and thus the molecular weight of such column-through fraction becomes smaller.

DISCUSSION

Chain Dimensions. The diameters of the complexed helices were consistently determined with SAXS and viscosity, and they agreed with each other, even though the physical natures of d and d_h are different. Upon the complexation, the diameter was slightly decreased from 2.6 to 2.2–2.4 nm for dA and was almost same or slightly decreased to 2.4–2.5 nm for S-dA. This change suggests that the complexation causes stretching of the helix.

The stretching due to the complexation was more significantly reflecting the change in M_L . As mentioned at Figure 3, if one-third of the tSPG is replaced by dA or S-dA without stretching, M_L should be increased by 1.15 or 1.17 times, respectively. The experimental results show that M_L of dA/SPG was almost the same as that of tSPG, and M_L of S-dA/SPG was smaller than that of tSPG. This is a concrete evidence for the helix stretching due to the complexation. Presuming that the observed rods consist of the stoichiometric composition, the helix pitch can be experimentally determined by the following equation, and the results are summarized in Table 1.

$$h = \frac{3M_{\text{dA}} + 2M_{\text{sSPG}}}{3M_L} \quad (4)$$

Here, M_{dA} and M_{sSPG} are the molar mass of dA_X and the single chain of SPG repeat units (313 for dA, 329 for S-dA, and 649 for SPG). Due to the complexation with dA, h was increased from 0.30 to 0.34–0.37 nm. For S-dA, it was further increased to 0.4 nm.

Uezu and co-workers have carried out MOPAC and MD calculations for poly(C)/SPG and complex.^{34,35} Their calculations indicate that the complex consists of two single SPG chains and one nucleotide chain and the hydrogen bonding array that was held in the center of the original triple helix of SPG between the second OH of the main chains glucoses is partially replaced by the complexed base molecule. We applied this method to dA/SPG and S-dA/SPG complexes and constructed the molecule models for both dA/SPG and S-dA/SPG (see the Supporting Information, S4) and obtained M_L , h , and the average chain diameters as listed in Table 1. According to their results, h was increased upon the complexation, which is consistent with our results.

Molecular Reason of Enhanced Stability of S-dA/SPG.

Recently, Mochizuki and co-workers^{16,17} found that S-dA/SPG shows about 20 °C higher dissociation temperature than dA/SPG. This finding surprised us. This is because the driving force of the complex formation is mainly the hydrogen bonding between the base molecule and the hydroxyl group on the second carbon of the main chain glucose, which has been deduced with the combination of MOPAC and MD calculations based on several experimental results, and the oxygen atoms of the phosphodiester bond are not directly involved in the complex formation. Their model shows that the phosphodiester moieties are located on the outer side of the helix and interact with the water molecules in solvent. Later, they found that the water molecules bound to the side chain of SPG play an important role of the chain stabilization. These molecules bind to two individual chains in the SPG helix and thus enforce the helix. They also found that due to the presence of these bound waters the helical pitch is changed. Refereeing these studies, we can suppose that the phosphor atom (or anion) in the S-dA/SPG may interact with the bond waters more preferably than the oxygen atom, and thus the stability is increased. If the water molecules bind two chains more tightly, the chains can come closer with each other, and thus the helix can elongate along the chain direction.

Chain Flexibility. The complexation dramatically decreases the persistence length. When dA₁₀₀ or dA₆₀ is complexed with two single SPG chains with $M = 130\text{K}$, the complex consists of a few of short dA chains, two for dA₁₀₀ and three for dA₆₀, and thus the complex has several of nicks. These nicks may decrease the persistence length. Additionally, polynucleotides have more free rotating chemical bonds to determine the chain conformation than polysaccharides, since only the 1–3 glycoside bond connecting the glucoses is such a bond in sSPG. The more freedom in poly(dA) should cause to decrease the persistence length. Compared with dA/SPG and S-dA/SPG, the latter shows a lower persistence length than the former. This could be related to the fact that the S-dA/SPG rod is thinner than dA/SPG.

CONCLUDING REMARKS

With the combination of the SEC/MALS plus viscometer and SAXS, the chain dimensions and the persistence length for the complexes were determined by use of the wormlike cylinder theories. The chain flexibility is reduced to almost 25% upon complexation for dA/SPG and to 15% for S-dA/SPG. This can be due to the presence of a nick or cooperating more flexible dA chain than sSPG. The changes in the molar mass per unit length and the diameter indicate that the helix is elongated or stretched along the axis direction upon the complexation. This feature is consistent with the molecular

simulation. Since the complexes containing antisense DNA and CpG motif are now under preclinical evaluation, the present information would be useful to fundamentally understand the complex in biological conditions.

■ ASSOCIATED CONTENT

S Supporting Information. Determination of the refractive index increments, comparison of the RI and UV chromatograms for S-dA60/SPG, AFM image, and calculation methods. This material is available free of charge via the Internet at <http://pubs.acs.org>.

■ AUTHOR INFORMATION

Corresponding Author

*E-mail: sakurai@env.kitakyu-u.ac.jp.

■ ACKNOWLEDGMENT

This work is financially supported by the JST CREST program, and all SAXS measurements were carried out at Spring-8 40B2 (2009A0012, 2009B1397, 2010A1089, 2010B1726).

■ REFERENCES

- (1) *Carbohydrate Biotechnology Protocols*; Bucke, C., Ed.; Methods in Biotechnology; Humana Press: Totowa, NJ, 1999.
- (2) *Biopolymers, Polysaccharides II: Polysaccharides from Eukaryotes*; Wiley-VCH: Berlin, NJ 2002; Vol. 6.
- (3) Norisuye, T.; Yanaki, T.; Fujita, H. Triple helix of a *Schizophyllum commune* polysaccharide in aqueous solution. *J. Polym. Sci., Polym. Phys. Ed.* **1980**, *18* (3), 547–558.
- (4) Kashiwagi, Y.; Norisuye, T.; Fujita, H. Triple helix of *Schizophyllum commune* polysaccharide in dilute solution. 4. Light scattering and viscosity in dilute aqueous sodium hydroxide. *Macromolecules* **1981**, *14* (5), 1220–1225.
- (5) Sato, S.; Sakurai, K.; Norisuye, T.; Fujita, H. Collapse of randomly coiled schizophyllan in mixture of water and dimethylsulfoxide. *Polym. J.* **1983**, *15*, 87–92.
- (6) Deslandes, Y.; Marchessault, R. H.; Sarko, A. Triple-helical structure of (1→3)- β -D-glucan. *Macromolecules* **1980**, *13* (6), 1466–1471.
- (7) Chuah, C. T.; Sarko, A.; Deslandes, Y.; Marchessault, R. H. Packing analysis of carbohydrates and polysaccharides. Part 14. Triple-helical crystalline structure of Curdlan and paramylon hydrates. *Macromolecules* **1983**, *16* (8), 1375–1382.
- (8) Stokke, B. T.; Elgsaeter, A.; Brant, D. A.; Kitamura, S. Supercoiling in circular triple-helical polysaccharides. *Macromolecules* **1991**, *24* (23), 6349–6351.
- (9) Stokke, B. T.; Elgsaeter, A.; Brant, D. A.; Kuge, T.; Kitamura, S. Macromolecular cyclization of (1→6)-branched-(1→3)- β -D-glucans observed after denaturation—renaturation of the triple-helical structure. *Biopolymers* **1993**, *33* (1), 193–198.
- (10) McIntire, T. M.; Brant, D. A. Observations of the (1→3)- β -D-glucan linear triple helix to macrocycle interconversion using non-contact atomic force microscopy. *J. Am. Chem. Soc.* **1998**, *120* (28), 6909–6919.
- (11) Sakurai, K.; Shinkai, S. Molecular recognition of adenine, cytosine, and uracil in a single-stranded RNA by a natural polysaccharide: Schizophyllan. *J. Am. Chem. Soc.* **2000**, *122* (18), 4520–4521.
- (12) Sakurai, K.; Mizu, M.; Shinkai, S. Polysaccharide–polynucleotide complexes. 2. Complementary polynucleotide mimic behavior of the natural polysaccharide schizophyllan in the macromolecular complex with single-stranded RNA and DNA. *Biomacromolecules* **2001**, *2* (3), 641–650.
- (13) Anada, T.; Okada, N.; Minari, J.; Karinaga, R.; Mizu, M.; Koumoto, K.; Shinkai, S.; Sakurai, K. CpG DNA/zymosan complex to enhance cytokine secretion owing to the cocktail effect. *Bioorg. Med. Chem. Lett.* **2006**, *16* (5), 1301–1304.
- (14) Koyama, S.; Aoshi, T.; Tanimoto, T.; Kumagai, Y.; Kobiyama, K.; Tougan, T.; Sakurai, K.; Coban, C.; Horii, T.; Akira, S.; Ishii, K. J. Plasmacytoid dendritic cells delineate immunogenicity of influenza vaccine subtypes. *Sci. Transl. Med.* **2010**, *2* (25), 25ra24.
- (15) Shimada, N.; Ishii, K. J.; Takeda, Y.; Coban, C.; Torii, Y.; Shinkai, S.; Akira, S.; Sakurai, K. A polysaccharide carrier to effectively deliver native phosphodiester CpG DNA to APCs. *Bioconjugate Chem.* **2007**, *18* (4), 1280–1286.
- (16) Minari, J.; Mochizuki, S.; Matsuzaki, T.; Adachi, Y.; Ohno, N.; Sakurai, K. Enhanced cytokine secretion from primary macrophages due to dextran-1 mediated uptake of CpG DNA/ β -1,3-glucan complex. *Bioconjugate Chem.* **2010**, *22* (1), 9–15.
- (17) Mochizuki, S.; Sakurai, K. β -1,3-Glucan/antisense oligonucleotide complex stabilized with phosphorothioation and its gene suppression. *Bioorg. Chem.* **2010**, *38* (6), 260–264.
- (18) Yanaki, T.; Norisuye, T.; Fujita, H. Triple helix of *Schizophyllum commune* polysaccharide in dilute solution. 3. Hydrodynamic properties in water. *Macromolecules* **1980**, *13* (6), 1462–1466.
- (19) Sato, T.; Norisuye, T.; Fujita, H. Triple helix of *Schizophyllum commune* polysaccharide in dilute solution. 5. Light scattering and refractometry in mixtures of water and dimethyl sulfoxide. *Macromolecules* **1983**, *16* (2), 185–189.
- (20) Yamakawa, H.; Fujii, M. Intrinsic viscosity of wormlike chains. Determination of the shift factor. *Macromolecules* **1974**, *7* (1), 128–135.
- (21) Yanaki, T.; Kojima, T.; Norisuye, T. Triple helix of scleroglucan in dilute aqueous sodium hydroxide. *Polym. J.* **1981**, *13*, 1135–1143.
- (22) Sletmoen, M.; Naess, S. N.; Stokke, B. T. Structure and stability of polynucleotide-(1, 3)-[β]-D-glucan complexes. *Carbohydr. Polym.* **2009**, *76* (3), 389–399.
- (23) Sletmoen, M.; Stokke, B. T. Structural properties of poly C-scleroglucan complexes. *Biopolymers* **2005**, *79* (3), 115–127.
- (24) Naruse, K.; Eguchi, K.; Akiba, I.; Sakurai, K.; Masunaga, H.; Ogawa, H.; Fossey, J. S. Flexibility and cross-sectional structure of an anionic dual-surfactant wormlike micelle explored with small-angle X-ray scattering coupled with contrast variation technique. *J. Phys. Chem. B* **2009**, *113* (30), 10222–10229.
- (25) Yamakawa, H.; Fujii, M. Light scattering from wormlike chains. Determination of the shift factor. *Macromolecules* **1974**, *7* (5), 649–654.
- (26) Yamakawa, H.; Fujii, M. Translational friction coefficient of wormlike chains. *Macromolecules* **1973**, *6* (3), 407–415.
- (27) Fujita, H. *Polymer Solutions*; Elsevier: Amsterdam, The Netherlands, 1990; Vol. 9.
- (28) Yamakawa, H.; Yoshizaki, T. Transport coefficients of helical wormlike chains. 3. Intrinsic viscosity. *Macromolecules* **1980**, *13* (3), 633–643.
- (29) Nakamura, Y.; Norisuye, T. Scattering function for wormlike chains with finite thickness. *J. Polym. Sci., Polym. Phys. Ed.* **2004**, *42*, 1398–1407.
- (30) Sakuragi, M.; Takeda, Y.; Shimada, N.; Sakurai, K. *Polym. Bull.* **2008**, *61* (1), 107–117.
- (31) Miyoshi, K.; Uezu, K.; Sakurai, K.; Shinkai, S. *Chem. Biodiversity* **2004**, *1* (6), 916–924.
- (32) Okobira, T.; Uezu, K.; Sakurai, K.; Shinkai, S. *Kabunshi Ronbunshu* **2011**, *68* (11), 711–718.
- (33) Roe, R. J. *Methods of X-ray and Neutron Scattering in Polymer Science*; Oxford University Press: Oxford, U.K., 2000.
- (34) Miyoshi, K.; Uezu, K.; Sakurai, K.; Shinkai, S. Polysaccharide–polynucleotide complexes. Part 32. Structural analysis of the Curdlan/poly(cytidylic acid) complex with semiempirical molecular orbital calculations. *Biomacromolecules* **2005**, *6* (3), 1540–1546.
- (35) Okobira, T.; Miyoshi, K.; Uezu, K.; Sakurai, K.; Shinkai, S. Molecular dynamics studies of side chain effect on the β -1,3-D-glucan triple helix in aqueous solution. *Biomacromolecules* **2008**, *9* (3), 783–788.

■ NOTE ADDED AFTER ASAP PUBLICATION

Figure 3 was updated; paper reposted 12/9/11.